Catalysis Today 149 (2010) 352–357

Contents lists available at ScienceDirect

Catalysis Today

journal homepage: www.elsevier.com/locate/cattod

Effect of Cu on Ni nanoparticles used for the generation of carbon nanotubes by catalytic cracking of methane

Ismael González [a,*], Juan Carlos De Jesus [a], Caribay Urbina de Navarro [b], Miguel García [b]

[a] *Laboratorio de Análisis de Superficies, PDVSA-INTEVEP, Los Teques 1201, Venezuela*

[b] *Centro de Microscopía Electrónica, Facultad de Ciencias, Universidad Central de Venezuela, 1040, Venezuela*

ARTICLE INFO

Article history:
Available online 26 August 2009

Keywords:
Carbon nanotubes
Ni catalyst
Ni nanoparticles
Methane catalytic cracking

ABSTRACT

In this study, a simple method for the addition of Cu to unsupported nickel nanoparticles is employed to investigate the promotion effect of copper during the nickel-catalyzed decomposition of methane into carbon nanotubes. Bulk nickel and copper acetates were mixed by grinding the parent salts in a mortar, to obtain samples with selected Ni/Cu atomic ratios ($NiCu_{0.03}$, $NiCu_{0.07}$ and $NiCu_{0.16}$) that were decomposed in situ on methane streams using a thermogravimetric analyzer (TGA). Weight increase was related quantitatively to the production of carbon nanotubes by catalytic cracking of methane, and the materials were complementary characterized ex situ by electron microscopy. The results suggest that copper most likely induces the disaggregation of nickel particles during the course of the catalytic cracking, but copper by itself was not effective to improve quantitatively the production of carbon nanotubes. In spite of very low methane conversions, good quality multiwalled carbon nanotubes are obtained and characterized by HRTEM.

1. Introduction

Carbon nanostructures formed as by-product during hydrocarbon decomposition can be used as a functional material, such as fibers, graphite, carbon black, composites, and electrodes. These materials have been an interesting research field in recent years due to their extraordinary physical and chemical properties. Some examples are the high strength, chemical purity and chemical inertness, which allow them be ideally used as supports in various catalytic heterogeneous processes, especially selective hydrogenation [1–3].

Today methane decomposition is one of the most environmentally attractive alternatives to produce pure hydrogen from natural gas (NG) [4–7]. The direct thermal decomposition of methane is an endothermic reaction, thermodynamically favored at elevated temperatures:

$$CH_4 \rightarrow C + 2H_2, \qquad \Delta H^\circ = 75.6\,\mathrm{kJ/mol}$$

Whatever the inlet methane concentration be, at atmospheric pressure and temperatures higher than 600 °C methane conversions higher than 60% can be achieved. Due to the high energy of the C–H bond (440 kJ/mol), higher temperatures are required (above 1200 °C) to activate this hydrocarbon [8]. This process produces directly hydrogen free of CO/CO_2, in comparison to conventional hydrogen production processes, e.g., steam methane reforming (SMR) and coal gasification, which require additional steps like water gas shift and CO_2 removal by adsorption [7,9].

Various transition metals, such as Fe and Co [10,11] have been widely used to catalyze methane decomposition, but conventionally due to its low cost and wide availability, Ni has been the most commonly used transition metal to conduct cracking, steam reforming and partial oxidation of methane [12–14]. Amorphous carbon produced initially as an undesirable by-product in most hydrocarbon conversion processes, severely impaired catalyst activity by blocking active metallic centers. However, especially during low conversion regimes, nickel catalyze hydrocarbon cracking producing steadily pure hydrogen together with highly organized nanostructured carbon, and under this circumstances it has been demonstrated that nickel particles can remain active during considerable intervals under very high carbon loadings.

Morphological appearance of the deposited nanostructured carbon depends mainly on the nature of the active sites of the catalyst [15], the structure of the catalytic system [16], and the textural properties and the size of the catalyst particles [17]. Additionally, these factors affect the kinetics of methane decomposition and hence the feasibility to obtain hydrogen. During the course of the catalytic cracking of hydrocarbons, it has been found that active nickel particles detach from the support in conventional heterogeneous catalysts, traveling at the tip of the carbon structures while the cracking reaction develops, making nickel much more tolerant to carbon. It is therefore logical to assume that the size of the metal nickel particle controls decisively the

---

[*] Corresponding author. Tel.: +58 212 3305802; fax: +58 212 3307230.
E-mail address: gonzaleziz@pdvsa.com (I. González).

0920-5861/$ – see front matter © 2009 Elsevier B.V. All rights reserved.
doi:10.1016/j.cattod.2009.07.101

diameter of the carbon nanostructures, and that smaller nickel nanoparticles will conduct the reaction more efficiently before encapsulation or agglomeration of the active phase take place.

Large scale and economically viable hydrocarbon cracking processes should find viable uses for the large amounts of nanostructured carbon that will be produced stoichiometrically with the CO_x-free hydrogen. Applications of carbon nanostructures are currently envisioned, among others, in the field of hydrogen storage [18], but usually purification of the carbon materials to detach the exhausted catalyst from the carbon matrix is needed. Separation of active metals is feasible by mild acid treatments [19], but complete removal of accompanying oxidic supports requires often more severe and potentially destructive treatments.

First suggestions of Ni feasibility to produce in a sustainable way hydrogen and novel carbon materials were reported by Muradov [4,20,21] and Parmon et al. [22]. Other studies about the use of nickel catalyst showed filamentous carbon production [23,24], at relatively low temperatures (550 °C), but with a low methane conversion (15%). Therefore, being Ni nanoparticles very active for the cracking reaction in the 500–600 °C interval, they usually decompose methane less efficiently at temperatures higher than 650 °C due to fast deactivation [25]. Today interest in catalytic cracking is therefore focused in developing catalysts with longer time on stream stability, and one frequent approach has been the promotion of active metallic nickel with other metals. Particularly, the role of copper in the promotion of metallic nickel for the catalytic cracking of hydrocarbons is somewhat controversial. For example, Li et al. [26] and Avdeeva et al. [27] showed that for Al_2O_3 supported nickel catalysts prepared by coprecipitation, the addition of copper is beneficial to improve cracking efficiency. Recently, Cunha et al. [28] have reviewed several studies pertinent to catalytic methane decomposition (CMD) on supported and unsupported Ni–Cu catalysts. The key finding is that promotion of Cu avoids the formation of encapsulating carbon species on active metal particles surfaces, allowing without restraint filamentous carbon formation which essentially does not deactivate the catalysts. The promotion in activity and selectivity is attributed to the dilution of the nickel surface atoms (geometric effect), rather than to an electronic effect. The formation of smaller ensembles of nickel surface atoms likely minimizes the interactions of amorphous adsorbed carbon species, thus reducing the rate of encapsulating carbon formation.

On the other hand, Chesnokov [29] and Takenaka et al. [25], studying nickel catalysts supported in MgO and SiO_2, respectively, found a negative effect of copper for the cracking reaction. With most results obtained so far employing heterogeneous catalysts, the effect of the support needs to be accounted for appropriately in order to understand the catalytic behavior of the active metal and the promotion effect of other metals during the catalytic cracking of hydrocarbons.

In a previous study, it was found that direct thermal decomposition of nickel acetate on an inert (He and N_2) gas atmosphere produces metallic nickel nanoparticles [30,31] with sizes ranging between 20 and 130 nm [31]. It was also found that the generation of ex-acetate nickel nanoparticles in methane streams in a thermogravimetric analyzer coupled to a quadrupole mass spectrometer is a convenient way to monitor in situ the catalytic activity of hydrocarbon cracking to produce hydrogen and multiwalled carbon nanotubes (MWCNT) [32]. The C to Ni atomic ratios (C/Ni or NiC_x) estimated directly from TGA data during in situ catalytic decomposition of methane may provide a systematic approach to assess the catalytic activity of pure and modified nickel nanoparticles, and eventually compare performances between supported and unsupported systems.

In this work, a simple thermogravimetric method for the preparation of unsupported Cu–Ni nanoparticles is proposed to investigate the promotion effect of copper during the nickel-catalyzed decomposition of methane into carbon nanotubes and hydrogen. We emphasized the characterization of the carbon nanostructures by transmission electron microscopy.

2. Experimental

2.1. Materials

Stoichiometric ratios of commercially available nickel acetate tetrahydrate $[Ni(CH_3CO_2)_2{\cdot}4H_2O]$ and copper acetate monohydrated $[Cu(CH_3CO_2)_2{\cdot}H_2O]$ were ground together using an agate mortar and pestle, to prepare homogeneous powders with nominal atomic compositions of $NiCu_{0.03}$, $NiCu_{0.07}$ and $NiCu_{0.16}$. Methane (99.9 wt%) and argon (99.9 wt%) were used as received.

2.2. Temperature-programmed methane reaction

Thermogravimetric analyses (TGA) were carried out on a NETZSCH STA 409 PC LUXX instrument. For each experience, about 15 mg of the homogeneous powders were loaded into a 5 ml alumina crucible, to allow extra room to keep metallic nanoparticles and carbon nanotubes completely inside the weighting area along the treatments. The initial gas mixture (CH_4:Ar) was supplied at all times at a constant flow rate of 70 ml/min, and 50% CH_4 concentration was regulated accurately employing mass flow controllers existing in a NETZSCH Pulse TA gas mixer. The heating rate was 20 °C/min for all the measurements, and a temperature range from 20 to 900 °C was chosen to probe the temperature-programmed reaction in a fixed concentration of 50% methane in Argon. The temperature range was selected to be between room temperature and 600–630 °C. At approximately 400 °C the acetate precursors are entirely transformed to metallic nanoparticles [30,31], and at this temperature the catalytic cracking of methane properly starts and continues until 600–630 °C, when the metallic nanoparticles are deactivated. The total conversion of methane is therefore estimated with the following formula:

$$XCH_4(\%) = \left(\frac{C_f - C_{NP}}{CH_{4\,\text{total}}}\right) \times 100$$

where XCH_4 (%) is the average methane conversion, C_f is the amount of carbon accumulated at the end of the reaction, C_{NP} is the amount of carbon remaining (usually less than 2%) after thermal decomposition of the acetate precursors [30,31], and $CH_{4\,\text{total}}$ is the total amount of methane flushed into the balance in the 400 to 600–630 °C range during the course of the active cracking reaction.

2.3. Transmission electron microscopy

Morphologic evaluation of carbon–nickel and carbon–copper–nickel residues was carried out in an electron transmission microscope (TEM), working at 100 kV accelerating voltage and a field emission electron transmission microscope (FE-HRTEM) operated at 200 kV accelerating voltage. Specimens were prepared by ultrasonic dispersion of the slightly grounded samples in a 40% ethanol–water solution, and then a drop of the suspension was applied to collodion graphite coated copper grids.

3. Results and discussion

3.1. Ex-acetates nanoparticles

Fig. 1 shows TEM images of residues collected after thermal decomposition at 400 °C of metal acetates in a stream of 50% of methane in argon, at 50 ml/min. A micrography of the residue of pure nickel acetate obtained from our previous study (Fig. 1a) [32] is compared with an equivalent nickel/copper mixture ($NiCu_{0.07}$)

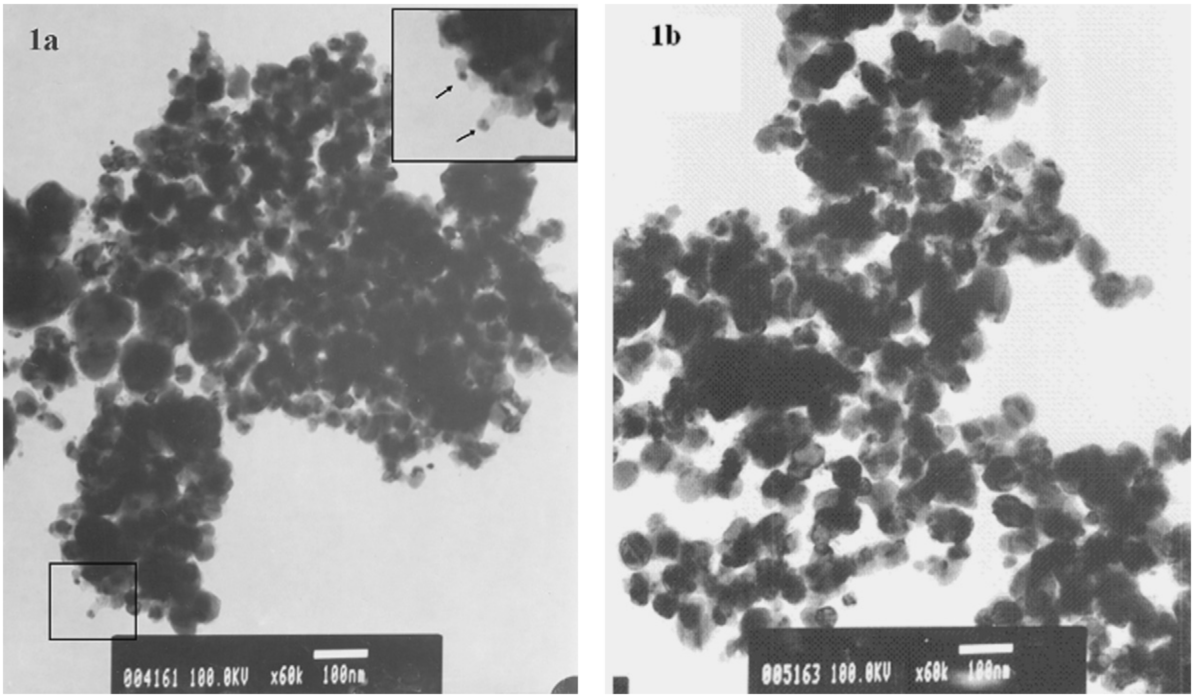

Fig. 1. Particles obtained at 400 °C on CH_4 stream for (a) Pure Ni and (b) $NiCu_{0.07}$.

produced in this work (Fig. 1b). Ni and NiCu particles shown in our TEM images seem to be around 100 nm, but we assume that this is due to insufficient dispersion during sample preparation and/or magnetic agglomeration [33]. Therefore, detailed size distribution and morphology analysis of nickel and nickel–copper ex-acetate particles were not attempted from the TEM results presented in Fig. 1. However, it is worth to mention here that incipient formation of carbon nanotubes was obvious at only 400 °C as we reported previously when pure nickel acetate is decomposed in methane (Fig. 1a) [32], but it was not possible to detect any early formation of carbon nanostructures in NiCu particles as depicted in Fig. 1b. As will be discussed below, copper addition by itself was not capable to improve quantitatively the formation of carbon nanotubes in the conditions of the present study.

3.2. *Temperature-programmed methane reaction*

Thermograms presented in Fig. 2, show the decomposition of the series of NiCu acetates, from 25 to 400 °C, in a stream of 50% of methane in argon, at 50 ml/min. Details of the procedure and interpretation of the curves have been reported previously [30,32]. Briefly, parent acetates are quickly decomposed in inert and/or CH_4 streams inside a TGA, giving Ni and NiCu nanoparticles at approximately 400 °C. Carbon buildup resulting from the catalytic cracking can be followed in situ by measuring weight gains in the corresponding thermograms, from 400 to 650 °C. At above 500 °C and up to 600 °C the carbon deposition is nearly linear, and above 600 °C we reported a temporary deactivation zone where carbon deposition is halted and no more methane decomposition is evident [32]. The C/metal atomic ratio ($NiCu_xC_y$) is easily calculated from the TGA data, from stoichiometric considerations. As clearly depicted in the traces shown in Fig. 2, the amount of carbon deposited in the residues collected at approximately 600–630 °C, when the metal nanoparticles are completely deactivated, decrease with the increase of the Cu/Ni atomic ratio.

This trend is shown more clearly in Fig. 3, where the final C/(Ni + Cu) atomic ratio of the residues and the methane conversion are plotted against the Cu/Ni atomic ratio of the initial

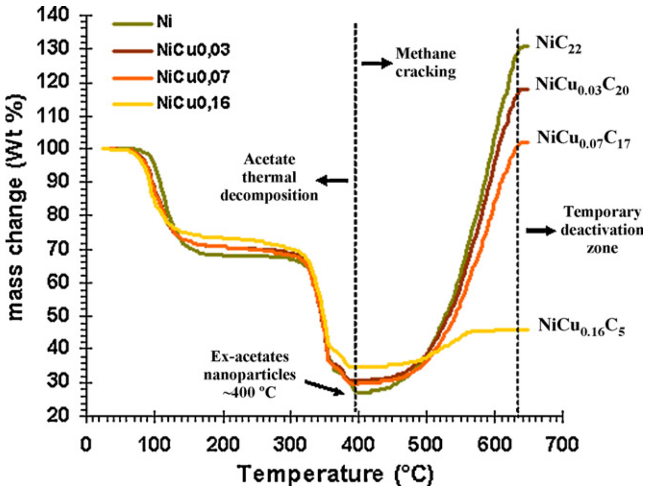

Fig. 2. TGA curves from methane decomposition runs.

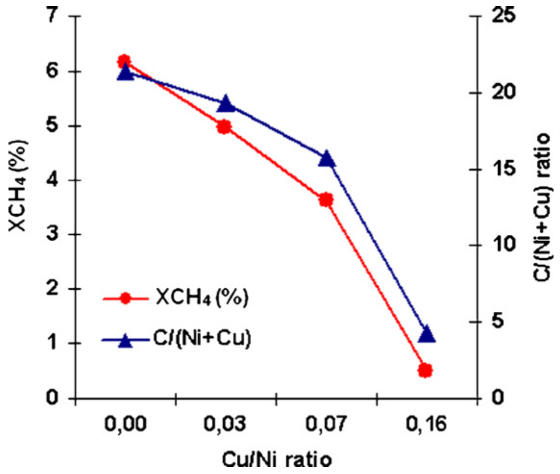

Fig. 3. Methane conversion and C/(Ni + Cu) atomic ratio vs. Cu/Ni atomic ratio of the catalytic particles.

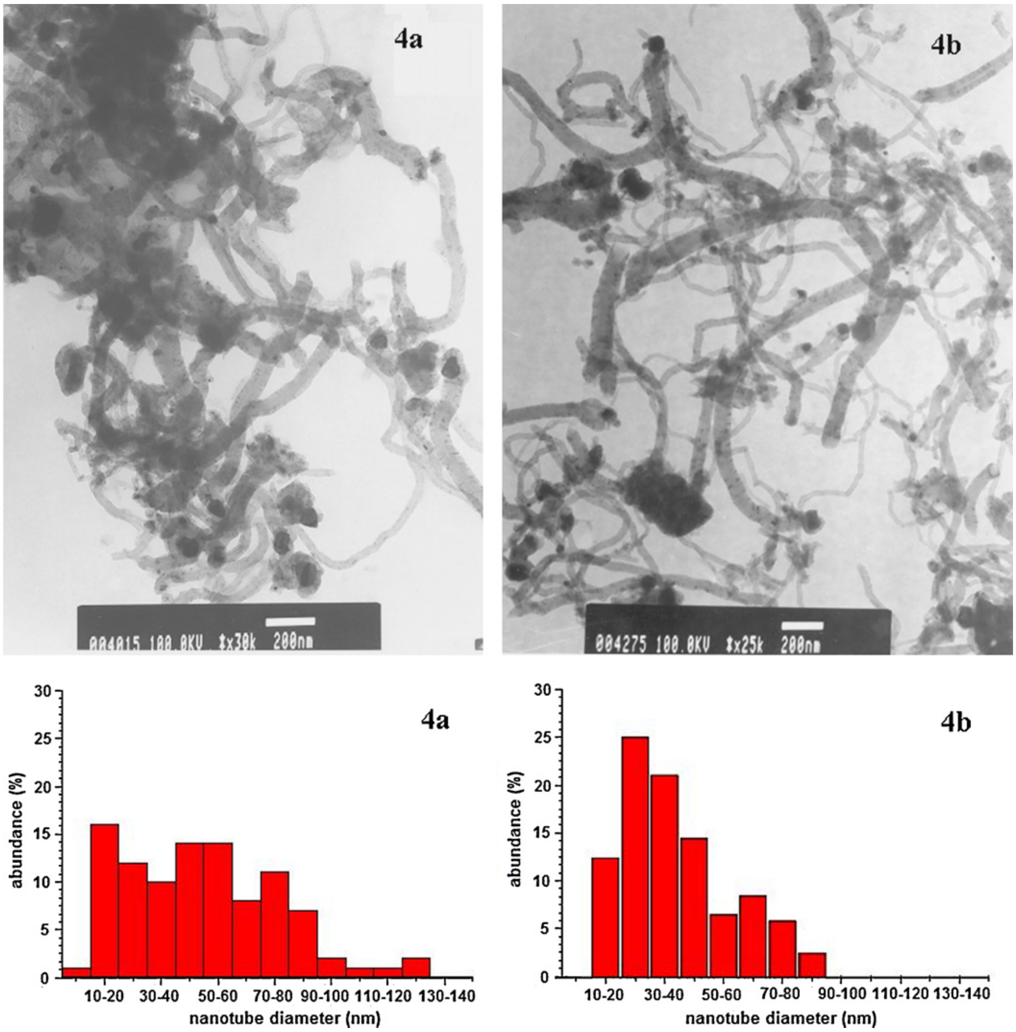

Fig. 4. TEM images and corresponding histograms of carbon nanotubes obtained from methane cracking employing pure Ni (a) and $NiCu_{0.07}$ (b) particles.

precursors. Clearly, the growth of carbon nanostructures in nickel particles was not enhanced by the addition of copper in the range of atomic concentrations employed in our study.

The best methane conversion attained in the present work was approximately 6% for pure nickel nanoparticles (see Fig. 3), conducing to a carbon deposition of 4.4 g-C/g-cat (C/(Ni + Cu) = 20). Avdeeva et al. [27] reported similar methane conversions and about double carbon deposition values in a vibrating flow reactor loaded with coprecipitated Ni–alumina and Ni–Cu–alumina catalysts. Low conversion regimes provide a long life of the active nanoparticles avoiding early deactivation and allowing the development of good quality carbon nanostructures, in a mild process with excellent analytical prospects to investigate catalytic performances. On the other hand, Suelves et al. [34] performed recently a literature comparison of some Ni–Cu based catalysts for catalytic cracking of methane, reporting carbon deposition values in the 39–404 g-C/g-cat range. The manufacture of exceptionally high carbon capacious catalysts is the key issue in the investigation of viable catalytic cracking processes, but it should be emphasized that as nearly all studies available in the open literature have been conducted typically with supported catalysts, complex metal–support interactions and changeable preparation and experimental conditions can make difficult a reliable understanding of all available information. We foresee

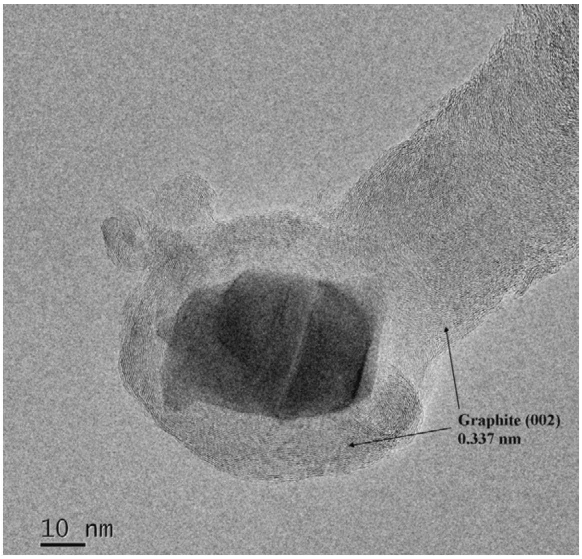

Fig. 5. HRTEM image of a Ni nanoparticle on the tip of a carbon nanotube obtained from methane decomposition on pure Ni sample.

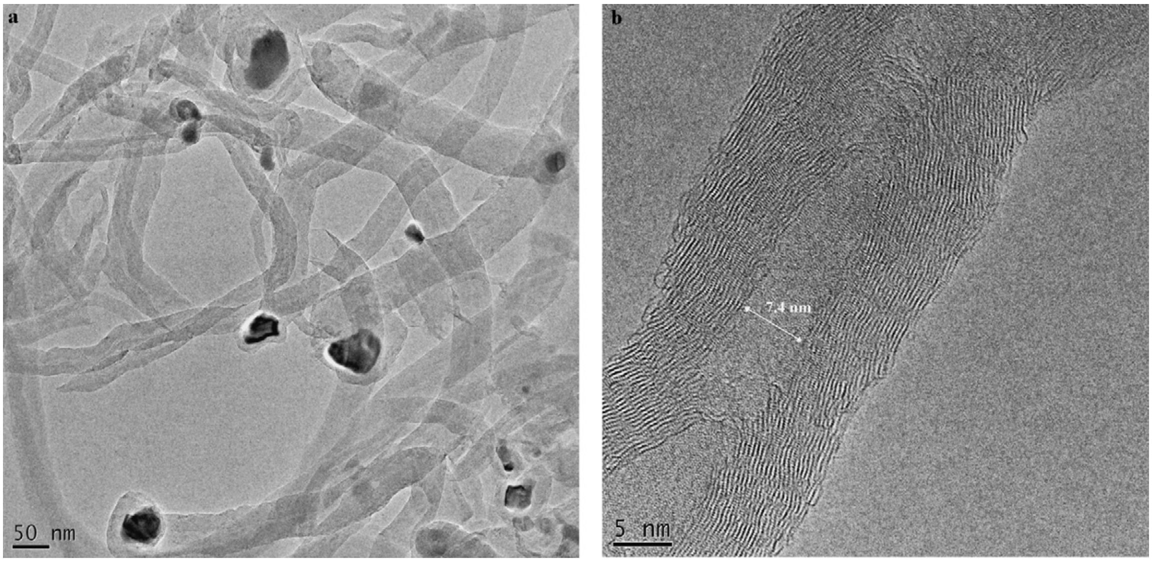

Fig. 6. (a) Images by HRTEM of carbon nanotubes obtained from methane catalytic decomposition on $NiCu_{0.07}$ nanoparticles. (b) Segment of a carbon tubular structure.

good prospects in the adoption of more specific studies employing isolated metal nanoparticles, in the way we put forward in the current study.

3.3. TEM and FE-HRTEM studies

Fig. 4 compares by TEM morphology and diameter distribution of carbon nanotubes (CNTs) obtained during methane cracking at 650 °C, employing pure Ni and $Ni/Cu_{0.07}$. Diameter distribution histograms are also presented in Fig. 4, measured by counting about 100 CNTs on the TEM images.

A large formation of CNTs with average diameter sizes between 50 and 60 nm is observed for pure Ni (Fig. 4a), but for $NiCu_{0.07}$ particles a bimodal diameter distribution with values centered in 20–30 nm and 60–70 nm was observed (Fig. 4b). This suggests that copper induces the disaggregation of the nickel particles in the course of methane cracking.

HRTEM images of carbon nanotubes and nanoparticles prepared in this study are shown in Figs. 5 and 6. Fig. 5 depicts a close view of a ~30 nm nickel nanoparticle located in the tip of a multiwalled carbon nanotube. The lattice fringes in the carbon structure surrounding the metallic nanoparticle match the (0 0 2) planes in pure graphite, as indicated by the arrows in Fig. 5.

Carbon nanotubes formed from catalytic methane decomposition using $NiCu_{0.07}$ particles were analyzed by HRTEM (Fig. 6a). Most of the metal nanoparticles are located at the end of the carbon nanotubes, which suggests a growth by the well-known tip mechanism [35]. Nanotubes present an average inner diameter between 7 and 8 nm, and in spite of minor defects or dislocations observed in the graphitic structures, the tubes show high crystallization in terms of availability of well-defined concentric graphene layers.

For the same $NiCu_{0.07}$ sample, a multiwalled tubular segment is observed in detail in Fig. 6b, where it can be noticed that the graphene layers are almost parallel to the tube axial direction in contrast with alternative carbon fishbone structures reported in many works where the grapheme planes are orientated at an angle of about 45° with respect to the angle of the fiber [36]. It is worth to mention here that CNTs samples prepared by the facile method reported in this work look remarkably pure from TEM and HRTEM images, and no other forms of carbon were observed, considering that all samples were characterized without further purification. This was particularly true in the present work for carbon nanotubes synthesized with Ni nanoparticles doped with Cu. It has been reported elsewhere that when the rate of carbon filament formation decreases upon Cu addition, the process of carbon atom aggregation becomes more ordered and, therefore, good quality and well-defined C nanotubes can be obtained [29].

4. Conclusions

Copper addition to nickel nanoparticles was not effective to improve quantitatively the production of carbon nanotubes by catalytic cracking of methane in unsupported catalysts prepared directly by physical mixing and thermal decomposition of acetate parent salts. Since practically most published results collected in supported catalysts assert a positive effect of copper for the promotion of catalytic hydrocarbon cracking in nickel, the inhibition effect observed in this work certainly deserves further development. Whether or not this difference is due to metal–support interactions or to a particular type of alloying between Cu and Ni in unsupported metallic nanoparticles will be addressed in future studies. However, our results suggest that copper induced the disaggregation of nickel particles during the course of the reaction, leading to the production of narrower carbon nanotubes. In spite of the low methane conversions attained in our experimental conditions, carbon nanotubes prepared in this study employing Ni and particularly Ni/Cu nanoparticles showed good quality and high crystallinity, as evidenced by the identification with HRTEM of well organized graphene layers. The reaction produced mainly multiwalled carbon nanotubes with inner average diameters of approximately 7–8 nm. We believe that the study of the reactivity of unsupported metal nanoparticles is an attractive approach to look into central catalytic aspects of hydrocarbon cracking reactions, avoiding complex aspects associated with supported counterparts.

References

[1] R.T.K. Baker, Carbon 27 (1989) 315.
[2] N.M. Rodríguez, J. Mater. Res. 8 (1993) 3233.
[3] K.P. de Jong, J.W. Geus, Catal. Rev. Sci. Eng. 42 (2000) 481.
[4] N. Muradov, J. Hydrogen Energy 18 (1993) 211.
[5] M. Steinberg, Int. J. Hydrogen Energy 24 (1999) 771.
[6] B. Gaudernack, S. Lynum, in: Proceedings of the 11th World Hydrogen Energy Conference, Stuttgart, Germany, (1996), p. 511.
[7] N. Muradov, Z. Chen, F. Smith, Int. J. Hydrogen Energy 30 (2005) 1149.

[8] P. Ammendola, R. Chirone, L. Lisi, G. Ruoppolo, G. Russo, J. Mol. Catal. A: Chem. 266 (2007) 31.
[9] S. Takenaka, H. Ogihara, I. Yamanaka, K. Otsuka, Appl. Catal. A 217 (2001) 101.
[10] H.J. Wang, E. Ruckenstein, Carbon 40 (2002) 1911.
[11] Y. Li, J. Chen, L. Chang, Appl. Catal. A: Gen. 163 (1997) 45.
[12] M.A. Ermakova, D.Y. Ermakov, Catal. Today 77 (2002) 225.
[13] T.V. Choudary, C. Sivadinarayana, C.C. Chusuei, A. Klinghoffer, D.W. Goodman, J. Catal. 199 (2001) 9.
[14] P. Wang, E. Tanabe, K. Ito, J. Jia, H. Morioka, T. Shishido, K. Takehira, Appl. Catal. A: Gen. 231 (2002) 35.
[15] V. Zaikovskii, V. Chesnokov, R. Buyanov, Kinetics Catal. 42 (6) (2001) 813.
[16] M.A. Ermakova, D.Y. Ermakov, A.L. Chuvilin, G.G. Kuvshinov, J. Catal. 201 (2001) 183.
[17] G.G. Kuvshinov, Y. Mogilnykh, D. Kuvshinov, D.Y. Ermakov, M.A. Ermakova, A. Salanov, N. Rudina, Carbon 37 (1999) 1239.
[18] A. Chambers, C. Park, R.T.K. Baker, N.M. Rodriguez, J. Phys. Chem. B 102 (1998) 4254.
[19] K. Otsuka, H. Ogilhara, S. Takenaka, Carbon 41 (2003) 223.
[20] N. Muradov, in: Proceedings of the 9th Miami International Congress on Energy and Environment, vol. 2, Miami Beach, FL, 1989.
[21] N. Muradov, Proc. HYPOTHESIS Internationa.l Symposium, Cassino-Gaeta, Italy, 1995.
[22] V.N. Parmon, G.G. Kuvshinov, V.A. Sobyanin, in: Proceedings of 11th World Hydrogen Energy Conference, Stuttgart, Germany, (1996), p. 697.
[23] M.A. Ermakova, D. Ermakov, G.G. Kuvshinov, L.M. Plyasova, J. Catal. 187 (1999) 77.
[24] M.A. Ermakova, D. Ermakov, G.G. Kuvshinov, Appl. Catal. A: Gen. 201 (2000) 61.
[25] S. Takenaka, Y. Shigeta, E. Tanabe, K. Otsuka, J. Catal. 220 (2003) 468.
[26] Y. Li, J. Chen, Y. Quin, L. Chang, Energy Fuels 14 (2000) 1188.
[27] L.B. Avdeeva, O.V. Goncharova, D.I. Kochubey, B.N. Novgorodov, L.M. Plyasova, Sh.K. Shaikhutdinov, Appl. Catal. A 141 (1996) 117.
[28] A.F. Cunha, J.J.M. Orfao, J.L. Figueiredo, Int. J. Hydrogen Energy 34 (2009) 4763 (and references therein).
[29] V. Chesnokov, V.I. Zaikovskii, R.A. Buyanov, V.V. Molchanov, L.M. Plyasova, Catal. Today 24 (1995) 265.
[30] J.C. De Jesús, I. González, A. Quevedo, T. Puerta, J. Mol. Catal. A: Chem. 228 (2005) 283.
[31] I. Gonzalez, J. Martinez, G. Jorge, J.C. De Jesus, C. Urbina, in: Proceedings of the 9th International American Congress of Electron Microscopy, La Habana, Cuba, 2005, No. M99.
[32] J.C. De Jesus, I. González, M. García, C. Urbina, J. Vac. Sci. Technol. A 26 (4) (2008) 913.
[33] Z. Wang, P. Xiao, N. He, Carbon 44 (2006) 3277.
[34] I. Suelves, J.L. Pinilla, M.J. Lázaro, R. Moliner, J.M. Palacios, J. Power Sources 192 (2009) 35.
[35] J.-W. Snoeck, G.F. Froment, M. Fowles, J. Catal. 169 (1997) 240.
[36] D. Chen, K. Christensen, E. Ochoa-Fernández, Z. Yu, B. Tøtdal, N. Latore, A. Monzon, A. Holmen, J. Catal. 229 (2005) 82.